Facile synthesis and thermal performances of stearic acid/titania core/shell nanocapsules by sol–gel method

Sara Tahan Latibari [a, *], Mohammad Mehrali [a, *], Mehdi Mehrali [a], Amalina Binti Muhammad Afifi [a], Teuku Meurah Indra Mahlia [b], Amir Reza Akhiani [a], Hendrik Simon Cornelis Metselaar [a, *]

[a] Department of Mechanical Engineering and Advanced Material Research Center, University of Malaya, 50603 Kuala Lumpur, Malaysia
[b] Department of Mechanical Engineering, Universiti Tenaga Nasional, 43009 Kajang, Selangor, Malaysia

ARTICLE INFO

Article history:
Received 14 September 2014
Received in revised form
26 February 2015
Accepted 2 April 2015
Available online 1 May 2015

Keywords:
Phase change material (PCM)
Nanoencapsulation
Stearic acid
Titanium dioxide
Sol–gel method

ABSTRACT

In order to improve the thermal properties of PCMs (phase change materials), in this study, a new series of NEPCMs (nanoencapsulated phase change materials) were synthesized using a sol–gel method with SA (stearic acid) as the core and TiO_2 (titania) as the shell material. The effects of the weight ratios of the SA/titania precursor TTIP (titanium tetraisopropoxide) on the morphology, thermal performance and thermal conductivity of the prepared nanocapsules are discussed. The experimental results indicate that the SA was encapsulated in spheres with minimum and maximum diameters of 583.4 and 946.4 nm, at encapsulation ratios between 30.36% and 64.76%. The results indicated that there was no chemical interaction between the core and shell materials, SA and TiO_2, which were compatible with each other under controlled synthesis conditions of pH 10. The NEPCMs with high mass ratios of SA/TTIP exhibited enhanced phase change properties and higher encapsulation efficiencies but lower thermal conductivities than NEPCMs with low mass ratios. Good thermal reliability and chemical stability of the NEPCMs were obtained by cycling the material through 2500 melting/solidifying cycles. In conclusion, the outstanding thermal stability and reliability of the prepared nanocapsules make these materials appropriate phase change materials for thermal energy storage applications.

1. Introduction

In recent years, renewable energy sources, such as solar energy, have emerged as suitable solutions to many environmental issues. These energy sources are intermittent by nature and require a storage system. One of the most significant storage systems is the TES (thermal energy storage) system, of which there are two types, SHTES (sensible heat thermal energy storage) and LHTES (latent heat thermal energy storage). PCMs (phase change materials) are among the latent heat storage system. Latent heat is stored in PCMs by storing phase transition heat at a nearly constant temperature [1]. For PCMs to be used in applications such as solar energy [2–4], smart textiles [5], heat transfer media [6,7], and intelligent buildings [8], the following characteristics are required: an appropriate phase change temperature, a superior melting enthalpy at the temperature under consideration, and a high density. PCMs must also be non-toxic, non-polluting and inexpensive [9].

PCMs are generally classified into three major types: organics (e.g., paraffins, fatty acids and esters), inorganics (e.g., salt hydrates and metallic alloys), and eutectics (mixtures of inorganics and/or organics) [10]. Among the PCMs studied, fatty acids, especially the linear chain fatty acid SA (stearic acid), have desirable characteristics including a suitable melting temperature, negligible supercooling through a phase change, thermal and chemical stability, outstanding phase transition performance, and non-toxicity. However, the direct employment of these organic PCMs for heat storage has several limitations because of the low thermal conductivity of PCMs, which leads to low charging and discharging rates and problems with leakage through the solid–liquid phase transition [11,12]. Several studies have been conducted to overcome these disadvantages. In recent years, there has been considerable interest in shape-stable composite PCMs [13,14] and encapsulation of PCMs within a solid shell [15]. The most beneficial objective for PCM (Phase Change Materials) microencapsulation would be to not only make PCMs easier and safer to use but also to

* Corresponding authors. Tel.: +60 3 79674451; fax: +60 3 79675317.
E-mail addresses: sara.tahan@siswa.um.edu.my (S. Tahan Latibari), mohamad.mehrali@siswa.um.edu.my (M. Mehrali), h.metselaar@um.edu.my (H.S.C. Metselaar).

http://dx.doi.org/10.1016/j.energy.2015.04.008
0360-5442/

decrease the reactivity of PCMs and enhance their thermal properties by increasing their heat transfer area [16,17]. Therefore, MEPCMs/NEPCMs (micro–/nanoencapsulated PCMs) have numerous benefits, such as preventing the leakage of melted PCMs, control of the volume change during a phase transition, and protection from damaging environmental interactions. These characteristics make NEPCMs more practical for energy storage applications, such as heat transfer, solar energy storage, building materials [18], and thermally regulated fibres and textiles [19]. The selection of appropriate shell materials for nanoencapsulation is important for controlling the properties of the micro–/nanocapsules. Polymers such as polyurethane and styrene-based copolymer [20] and Urea and formaldehyde [21] are used as the shell material in typical micro/nanocapsules of PCMs. These polymeric wall materials play a crucial role in enhancing the structural stability and permeability of PCMs [22]. Various physical and chemical approaches have been developed for micro–/nanoencapsulation, such as interfacial polymerisation [23,24], in situ polymerisation [25,26], suspension polymerisation [27], and spray drying [28]. Nevertheless, the flammability, toxicity, low thermal conductivity and inadequate thermal and chemical stability of MEPCMs limit their usage in polymeric shells. Therefore, organic-inorganic MEPCM composites have been receiving significant consideration [29]. It is well known that the thermal conductivities of inorganic materials are definitely higher than those of organic materials. Furthermore, the vast majority of inorganic materials exhibited enhanced rigidity and durability over those of polymeric materials; thus, an inorganic shell material with superior strength not only enhances the thermal transfer performance of the PCM system but also improves the durability and working reliability of MEPCMs [30,31]. Thus far, several methods have been used for the micro-/nanoencapsulation of organic PCMs into inorganic shells, such as the sol–gel method using an O/W (oil-in-water) emulsion route [32] and in situ interfacial polycondensation [33]. Li et al. [29] and Fang et al. [21] prepared paraffin microcapsules in a silica shell via in situ polycondensation and investigated the corresponding phase-change properties. In a previous study, we used the sol–gel technique to produce homogenous NEPCMs of PA (palmitic acid) in a SiO_2 shell. The effect of the synthesis conditions on the morphology and thermal properties of NEPCMs were studied [34]. In another work, we synthesized the microcapsules of palmitic acid within an aluminum hydroxide oxide shell. The thermal properties of the prepared microcapsules ascertain the applicability of them in thermal energy storage applications [35]. Lin et al. reported a novel MEPCM using AlOOH as the shell material; however, the MEPCM had a low latent heat value [36]. Shiyu et al. also successfully synthesised well-defined PCM microcapsules with an n-octadecane core and a silica shell, which exhibited a substantially enhanced thermal conductivity and phase-change performance [18]. In another study, Shiyu et al. reported the synthesis of n-octadecane microcapsules via a self-assembly technique in which $CaCO_3$ (calcium carbonate) was used as the shell material. The resulting $CaCO_3$-encapsulated PCM demonstrated a high thermal conductivity and durability as well as good phase-change performance because of the high mechanical strength of the shell material [22].

Few research studies have been conducted on the micro-/nanoencapsulation of fatty acids. The functional group of fatty acids makes the micro–/nanoencapsulation process more difficult to control than for paraffins. In addition, MEPCMs with more rigid shells must be produced to prevent the leakage of core material over numerous thermal cycles. A TiO_2 shell is rigid and can increase the thermal stability of the micro–/nanocapsules. Lei Cao et al. synthesised micro-/nanoencapsulated paraffin [37] and PA (palmitic acid) [38] using TiO_2 (titanium dioxide) shells. The authors prepared the MEPCMs using tetra-n-butyl titanate as a precursor in a sol–gel method under acidic conditions. The paraffin and PA were encapsulated in micro–/nanocapsules with diameters of approximately 50 and 200–400 nm, respectively, in an acidic environment. The encapsulation ratios of the paraffin micro–/nanocapsules was approximately 87% and for PA micro–/nanocapsules were 30% [37,38]. In MEPCM-dispersed thermal fluids, large microcapsules increase the fluid viscosity; thus, smaller MEPCMs must be developed or NEPCMs must be used [26]. Furthermore, higher encapsulation ratios enhance the energy storage properties of the MEPCMs. Therefore, both parameters are important and should be optimised. However, the synthesis and investigation of the thermal properties of nanoencapsulated SA with a TiO_2 shell has not been reported [30]. Thus, the purpose of this study is to develop a feasible encapsulation procedure for SA using a sol–gel process and to determine the synthesis conditions that optimise the microstructure, crystallisation behaviour and phase-change efficiency of the products.

2. Experimental section

2.1. Materials

The following chemicals were obtained from Fisher Scientific Inc. and used in the synthesis of the nanocapsules: SA ($C_{18}H_{36}O_2$, commercial grade, 99%), which was used as the organic PCM (core); sodium dodecyl sulphate (SDS, $NaC_{12}H_{25}SO_4$), which was used as the surfactant; titanium tetraisopropoxide (TTIP, $C_{12}H_{28}O_4Ti$, 98%), as the precursor for TiO_2; and absolute ethanol (C_2H_6O, 99.9%) and distilled water, which were used as solvents. The pH was adjusted using ammonium hydroxide (NH_4OH, 28%). All of the materials were chemically pure grade and were used as received.

2.2. Preparation of SA/TiO_2 NEPCMs

In the synthesis procedure, the O/W emulsion was prepared by mixing 0.3 g of SDS and 50 mL of distilled water using a magnetic stirrer at 1000 rpm. Once the temperature of the mixture stabilised at 70 °C, three g of SA was added to the mixture, and the emulsion was stirred under continuous agitation at the constant temperature of 70 °C for 1 h. After the SA was uniformly dispersed in the emulsion, 15 mL of absolute ethanol was added to the mixture.

The precursor solution was prepared in a separate beaker by mixing 15 mL of anhydrous ethanol with TTIP in the ratios listed in Table 1 for 15 min. Afterward, ammonium hydroxide was used to adjust the pH to 10, 10.8, and 11.5.

Nanocapsule formation was achieved in the last phase by adding the precursor solution dropwise into the SA emulsion while the emulsion was stirring continuously at 750 rpm at a temperature of 70 °C. After 2 h, the mixture was cooled to room temperature and washed with distilled water 3 times, and the resulting white powder was collected and dried in an oven at 50 °C. Twelve types of nanocapsules were obtained, as listed in Table 1.

2.3. NEPCM synthesis

The SA/TiO_2 nanocapsules were synthesised via polycondensation using a sol–gel route. In the first step, the oily SA was dispersed in an aqueous solution containing SDS as the surfactant. A typical O/W emulsion was obtained. In this case, the hydrophobic segments of the SDS were intermittently collocated with the hydrophilic segments of the SA molecules, and water molecules attached to the hydrophilic segments of the SA molecules. Thus, the hydrophobic SDS segments covered the surface of the SA droplets. After formation of the SA micelles, absolute ethanol was added as

Table 1
Chemical composition of the O/W emulsion and precursor solution used for the fabrication of NEPCMs.

		Precursor solution		
Sample number	SA/TTIP ratio (wt/wt)	TTIP (g)	Volume of absolute ethanol added (mL)	pH
ST1	50/50	3.00	15	10.0
ST2	60/40	2.00	15	10.0
ST3	70/30	1.28	15	10.0
ST4	80/20	0.75	15	10.0
ST5	50/50	3.00	15	10.8
ST6	60/40	2.00	15	10.8
ST7	70/30	1.28	15	10.8
ST8	80/20	0.75	15	10.8
ST9	50/50	3.00	15	11.5
ST10	60/40	2.00	15	11.5
ST11	70/30	1.28	15	11.5
ST12	80/20	0.75	15	11.5

an assistant emulsifier, which decreased the hydrolysis and condensation rate of the precursors in a subsequent step for optimising NEPCM formation. A transparent solution of TTIP and absolute ethanol was formed and used to modify the TTIP. Ammonium hydroxide (which contained water molecules) was added as a catalyst to initiate the hydrolysis reaction, and a transparent sol formed. In the final phase, a transparent sol of titania was added dropwise to the O/W emulsion, and the titania precursors were attracted to the surface of the SA micelles via the hydrogen bonding interaction between the titania precursors and hydrophilic sections of the SDS. Polycondensation of the Ti–OH bonds then occurred in the presence of water molecules under alkaline conditions, and a titania gel was formed around the SA micelle. Polycondensation of the titania resulted in the fabrication of compact titania shells over the surface of the SA droplets. Fig. 1 is a schematic of the entire NEPCM formation process.

2.4. Analytical methods

The chemical structure of the NEPCMs was analysed before and after thermal cycling using a Fourier transform infrared spectrometer (FTIR, Perkin Elmer-spectrum100 model) over the wavelength range of 450–4000 cm^{-1}. The crystallography of the nanocapsules was investigated using an X-ray diffractometer (XRD, EMPYREAN PANALYTICAL). A high-resolution FEI Quanta 200F SEM (scanning electron microscope) was used to observe and analyse the surface morphology and size of the SA nanocapsules. The surface elemental analysis was carried out by EDS (energy-dispersive X-ray spectrometry). The core and shell structure of the nanocapsules was observed using a transmission electron microscope (TEM-CARL ZEISS-LIBRA 120). The phase-change properties of pure SA and the prepared NEPCMs, such as the melting and freezing temperatures and latent heats, were obtained using a differential scanning calorimeter (Mettler Toledo-DSC 820C-Error ± 0.25–1 °C) at a heating rate of 5 °C/min in a purified nitrogen atmosphere. A thermogravimetric analysis (SETSYS Evolution TGA-SETARAM-Error ±0.02 μg) was performed at a heating rate of 10 °C/min and a temperature of 50–500 °C in purified nitrogen to obtain the weight loss and thermal stability of the SA and NEPCMs. The thermal conductivity of the nanocapsules was measured using a laser flash technique (Netzsch LFA 447 NanoFlash-Error less than % 3) at 35 °C using standard-sized samples. The thermal reliability of

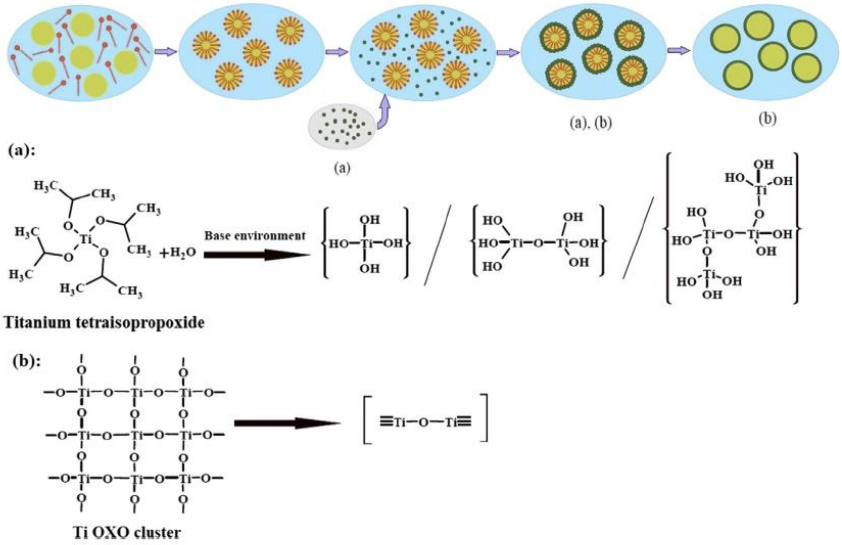

Fig. 1. Schematic of the nanoencapsulation of a titania shell with an SA core.

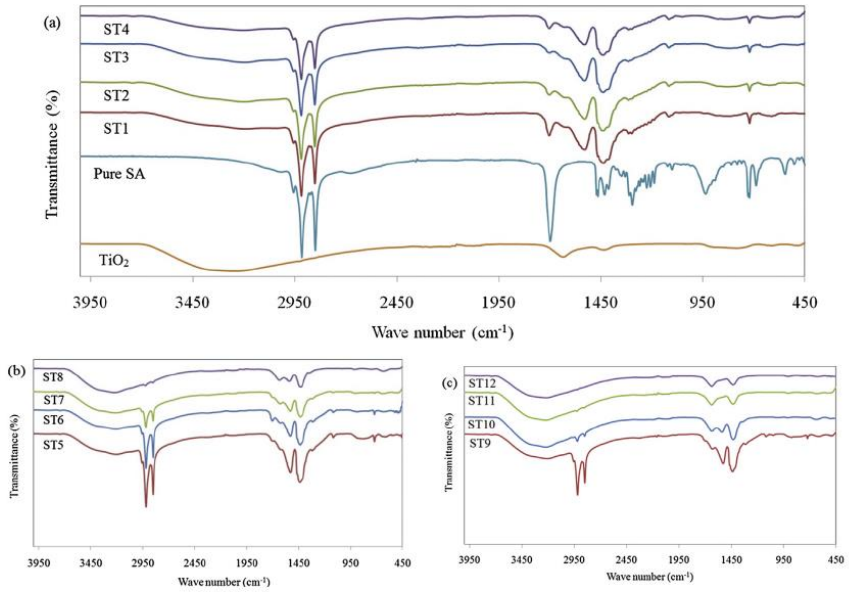

Fig. 2. FTIR spectra of TiO_2, pure SA, and NEPCMs synthesised at (a) pH 10, (b) pH 10.8, and (c) pH 11.5.

the nanocapsules during the melting and freezing processes was investigated by performing an accelerated thermal cycling test with an in-house thermal cycling system design (University of Malaya) [39]. The thermal cycling system was designed to operate at heating and cooling cycles between 30 °C and 80 °C. Up to 2500 thermal cycles were carried out, and the temperature variations of the nanocapsules were automatically recorded with an accuracy of ± 0.1 °C.

3. Results and discussion

3.1. Chemical characterization of NEPCMs

The chemical interaction between SA and TiO_2 affects the latent heat storage performance of the NEPCMs; thus, chemical, structural and stability analyses are important in evaluating the performance of NEPCMs. FT-IR spectroscopy was used to investigate the interaction between SA and TiO_2, as shown in Fig. 2. Fig. 2a shows the spectrum of SA plus the prepared TiO_2 sol. In the pure SA spectrum, the registered peak at 2915 cm^{-1} corresponded to the symmetrical stretching vibration of the C—H_3 group, and the peak at 2848 cm^{-1} corresponded to the symmetrical stretching vibration of the C—H_2 group. The stretching vibration of the C=O group produced a strong absorption peak at 1692 cm^{-1}. The peaks at 1461 and 1290 cm^{-1} were allocated to the in-plane bending vibration of the functional O—H group in SA, and the peak at 926 cm^{-1} corresponded to the out-of-plane bending vibration of the O—H functional group. The peak at 719 cm^{-1} corresponded to the in-plane swinging vibration of the O—H functional group [40]. In the TiO_2 spectrum, the absorption broad bands from approximately 2670 to 3800 cm^{-1} corresponded to the stretching and deformation vibrations of the —OH functional group in H_2O that were associated with absorbed water. The other peak at 1651 cm^{-1} corresponded to the stretching of titanium carboxylate that formed from the TTIP and ethanol precursors.

Fig. 2a shows the spectra for the ST1-ST4 samples that were prepared at pH 10 for different SA/TTIP mass ratios: the characteristic peaks of SA and TiO_2 were clearly distinguishable in the spectra of nanocapsules, and no peak shifts were observed. Furthermore, the absorption peak at 1539 cm^{-1} in the spectra of the NEPCMs corresponded to the stretching vibration of the C=O from the small amount of titanium stearate that formed in the NEPCMs. The spectra of ST1-ST4 confirmed the successful encapsulation of SA by the titania shells. However, the characteristic peaks of SA did not appear in the spectra for the ST8 and ST10—ST12 samples (Fig. 2b, c), which were synthesized at pH values of 10.8 and 11.5. This result indicated that the SA encapsulation was not successful for the conditions under which these samples were prepared. The SEM images of these samples also confirmed this result. This result may have occurred because of an accelerated hydrolysis rate at higher pH values that did not allow sufficient time for encapsulation. Thus, all of the imaging results and analyses on ST1—ST4

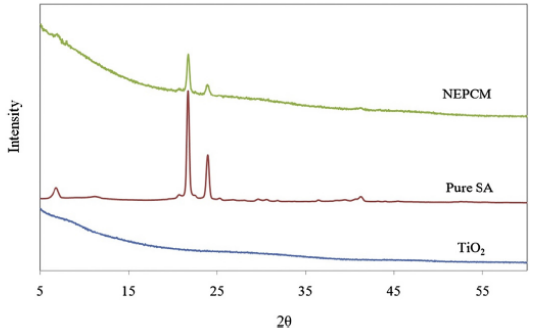

Fig. 3. XRD patterns of the TiO_2, pure SA and SA/TiO_2 NEPCMs.

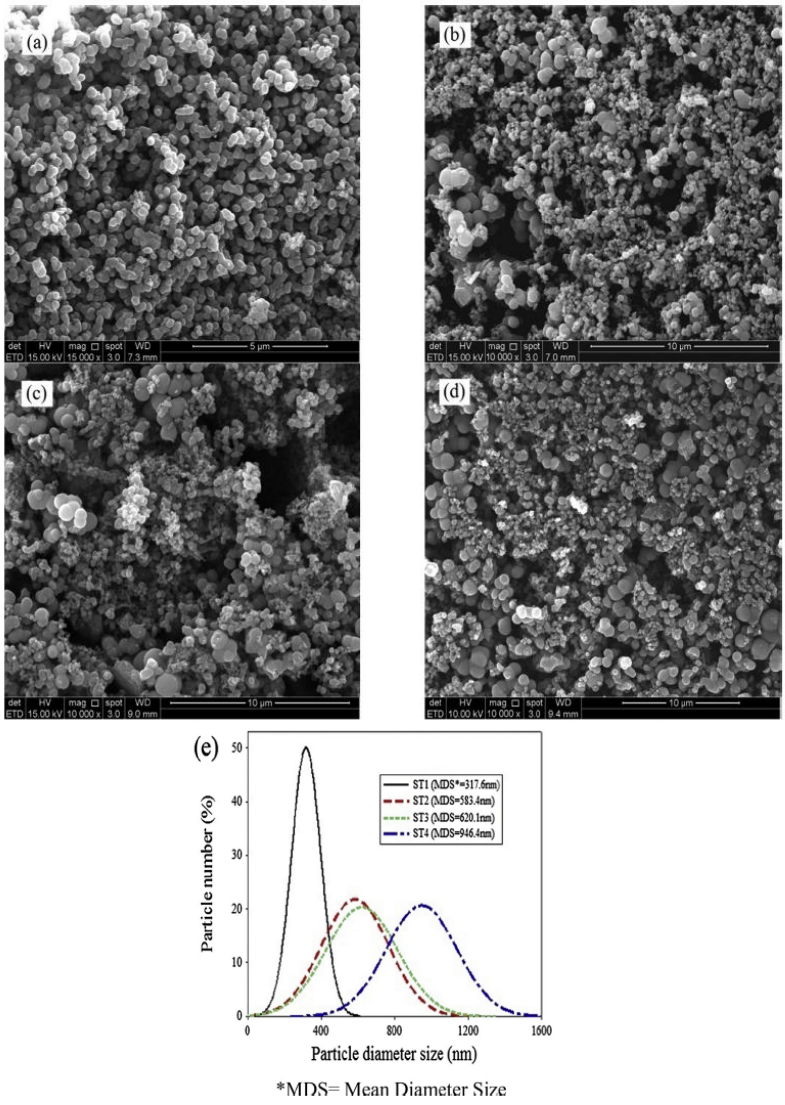

Fig. 4. SEM images for SA/TiO_2 nanocapsules for (a) ST1, (b) ST2, (c) ST3 and (d) ST4 and (e) particles size distributions of the prepared samples.

indicated that the NEPCMs were properly encapsulated at pH value of 10 that can be used to investigate the effect of the SA/TTIP mass ratios on the thermal properties of the NEPCMs.

3.2. Crystallography of NEPCMs

The XRD patterns of SA, the TiO_2 sol, and ST1 are shown in Fig. 3. The same XRD peaks were observed in the ST2, ST3, and ST4 patterns as for ST1 but at higher intensities because ST2, ST3, and ST4 contained higher amounts of SA than ST1. The SA peaks at 21.6° and 23.8° in Fig. 3 corresponded to the regular crystal structure of SA. No distinct XRD pattern can be observed in Fig. 3, indicating that the TiO_2 sol that was prepared by hydrolysis and condensation was non-crystalline and amorphous, which also explains the absence of the TiO_2 peaks from the NEPCM spectrum.

The NEPCM spectrum consisted of SA peaks superimposed on an amorphous bump for TiO_2. This result demonstrated that the crystal structure of the SA in the NEPCMs was not affected by the synthesis process and that SA was encapsulated in the TiO_2 shells because TiO_2 could not form inside the SA droplet. The decreased intensity of the XRD peaks of SA for ST1 compared to that for pure SA indicated that the SA crystallite size was smaller for the NEPCMs than for ST1 because SA crystal growth was inhibited by the small volume of the NEPCM capsules, which also increased the peak width.

Link to full text journal article :

http://www.sciencedirect.com/science/article/pii/S0360544215004260

https://ideas.repec.org/a/eee/energy/v85y2015icp635-644.html